

# Porosity, Underfill and Magnesium Loss during Continuous Wave Nd:YAG Laser Welding of Thin Plates of Aluminum Alloys 5182 and 5754

*Keyhole stability is found to play a major role in porosity formation*

BY M. PASTOR, H. ZHAO, R. P. MARTUKANITZ AND T. DEBROY

**ABSTRACT.** The influence of various welding parameters on porosity and underfill formation and magnesium loss during continuous wave Nd:YAG laser beam welding of thin plates of aluminum-magnesium Alloys 5182 and 5754 was investigated. The porosity within the welds was characterized by radiography, optical microscopy and SEM. The compositional change in the welds was measured by electron microprobe analysis.

The experimental results showed that the instability of the keyhole was the dominant cause of macro-porosity formation during laser welding of thin plates of aluminum Alloys 5182 and 5754. Hydrogen did not play a significant role in porosity formation. Although underfill was commonly observed at the root of full-penetration welds, sharp or deep notches, which are harmful to the mechanical properties of the welds, were not present. Reduction in magnesium concentration was more pronounced during conduction mode welding. Welding in keyhole mode resulted in much larger weld pool and less pronounced composition change. The extent of defocusing of the laser beam greatly affected the stability of the keyhole, weld pool geometry, pore formation and composition change.

## Introduction

The U.S. automotive industry is currently facing increased demands to simultaneously increase its fleet average fuel economy and reduce greenhouse gas emissions. In order to meet these new standards, the industry is increasingly moving toward decreasing the weight of the vehicles through the use of new materials, especially lightweight aluminum

alloys (Ref. 1). One of the major factors in their implementation involves the ability to fabricate, easily and reproducibly, structurally sound and defect-free welds. Laser beam welding is particularly critical to reduce the weight of the body structure through increased use of aluminum alloys and tailor welded blanks.

Porosity, loss of alloying elements and, for some heat treatable aluminum alloys, solidification cracking are the most common problems encountered in the laser welding of these alloys. The poor coupling between aluminum alloys and the laser beam is another major concern. Aluminum alloys absorb the laser more efficiently as the laser wavelength decreases (Ref. 2). Duley (Ref. 3) reported that the Nd:YAG laser with a characteristic wavelength of 1.06  $\mu\text{m}$  provided better coupling with aluminum than the CO<sub>2</sub> laser, which has a characteristic wavelength of 10.6  $\mu\text{m}$ . Furthermore, the absorption of the laser beam increases drastically when a keyhole is formed due to multiple reflections of the beam in the keyhole (Ref. 4). A Nd:YAG laser is therefore more attractive for the welding of aluminum alloys.

The detrimental effect of porosity on the mechanical properties of aluminum welds has been documented in the literature (Refs. 5–7). However, the mechanism of porosity formation during laser

beam welding is less well understood. Pore formation has been linked to hydrogen rejection from the solid phase during solidification (Refs. 8–11), imperfect collapse of the keyhole (Refs. 8, 12–14) and turbulent flow in the weld pool (Ref. 15). Sources of hydrogen in the weld metal include the filler metal and, to a lesser extent, the shielding gas and the base metal (Ref. 16). Woods (Ref. 11) showed that porosity does not form when the hydrogen content in aluminum alloys is lower than a threshold level. The threshold level varies for different aluminum alloys due to their differences in hydrogen solubility. Therefore, controlling the hydrogen content in the metal to below the threshold level can effectively control hydrogen porosity. However, severe porosity has been observed consistently (Ref. 17) during autogenous laser welding of aluminum alloys even when hydrogen contamination was minimized from the three known sources. Therefore, imperfect collapse of the keyhole and/or turbulent flow in the weld pool are important causes of porosity during laser welding of aluminum alloys.

Loss of volatile alloying elements, such as magnesium and zinc, due to selective vaporization is a common occurrence in the laser welding of aluminum alloys (Refs. 18–22). Automotive aluminum alloys are either solid-solution strengthened, such as the Al-5xxx alloys containing magnesium, or precipitation strengthened, such as Al-6xxx alloys containing Mg<sub>2</sub>Si. Loss of magnesium during the laser welding of Al-5xxx and Al-6xxx alloys may affect the degree of strengthening and cause degradation of the mechanical properties of these alloys. The change in weld metal composition depends on the vaporization rate and the volume of the weld pool (Refs. 23, 24). Although the rate of vaporization increases with laser power, the change in composition is most pronounced at low powers because of the small size and, consequently, the high surface-to-vol-

## KEY WORDS

Nd:YAG  
Lasers  
Welding  
Porosity  
Underfill  
Aluminum  
Keyhole Mode  
Thin Plate

M. PASTOR, H. ZHAO, R. P. MARTUKANITZ and T. DEBROY are with the Department of Materials Science and Engineering, The Pennsylvania State University, University Park, Pa.



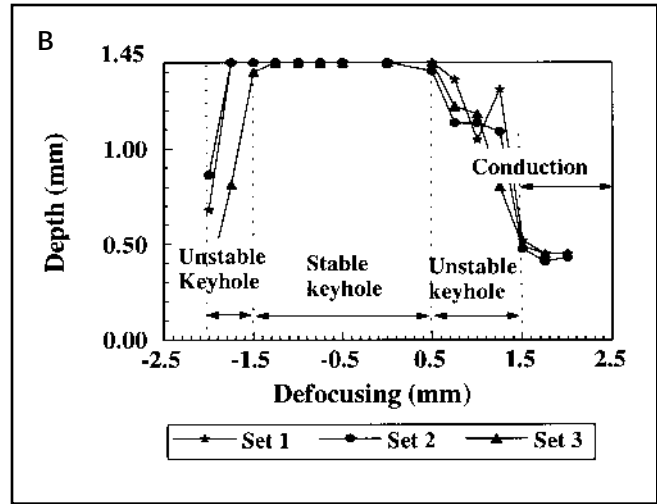
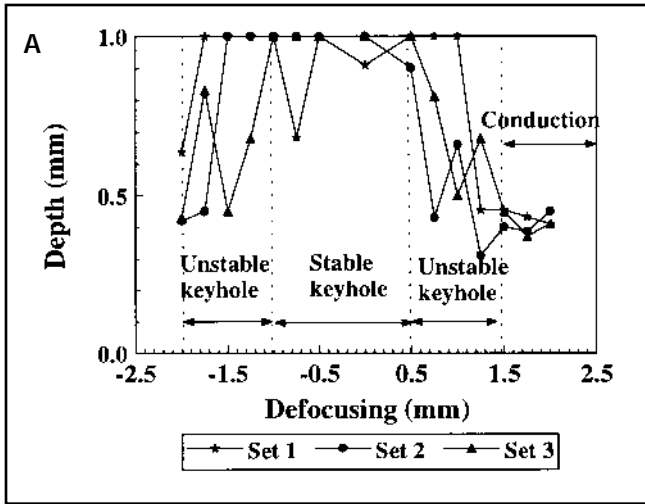


Fig. 3 — Depth of penetration in laser welded aluminum alloys at several defocus values. A — 5182; B — 5754. Nominal power 3 kW, welding speeds 250 in./min (105.8 mm/s) and 150 in./min (63.5 mm/s) for Alloys 5182 and 5754, respectively, and shielding gas flow rate 200 ft<sup>3</sup>/h (5.66 m<sup>3</sup>/h) of helium.

livered to the workpiece. The beam was delivered using a 600- $\mu$ m diameter fiber of fused silica to a f2 focus optics manipulated through a micropositioning stage mounted on a linear translation device. The focal length of the f2 optics for Nd:YAG laser is 77.7 mm. The beam radius at the focal point is 300  $\mu$ m. The beam was provided at a 75-deg forward angle relative to the workpiece to prevent damage to the optics due to back reflection. An ancillary copper nozzle having a 8.0-mm inside diameter was utilized to provide shielding gas. This gas nozzle was directed opposite to the direction of travel at an angle of 30 deg with the workpiece. During welding, the aluminum plates were placed horizontally on a copper back plate. The back plate had a U-shaped groove of 2.0-mm width and 1.5-mm depth under the weld region. Therefore, the liquid metal was not supported by the back plate. Helium was used as the shielding gas. Because of its high thermal conductivity, helium can easily conduct heat away from the plasma plume and keep the plasma volume small.

The effect of laser beam defocusing was evaluated by altering the distance between the workpiece and the optics to obtain defocusing distances ranging from -2.0 mm to +2.0 mm. The variation of beam radius and power density with distance from the focal point is given in the appendix. The focal point position of the Nd:YAG laser was determined with the help of a He-Ne red diode focusing laser whose focal length was 0.104 in. (2.64 mm) shorter than that of the Nd:YAG laser. A stainless steel plate of 0.104-in. thickness was placed on the specimen table and its elevation was adjusted to focus the He-Ne laser on the stainless

steel plate surface. The original specimen table surface without the stainless steel plate was taken as the focal point for the Nd:YAG laser. A nomenclature of positive defocusing to represent the focal point to be above the top surface of the workpiece and negative defocusing to represent the focal point to be below the top surface will be used throughout this paper. The effect of travel speed on weld characteristics was also investigated by varying the travel speed of the laser beam from 125 to 300 in./min (52.9 to 127 mm/s).

To examine the effect of hydrogen on porosity formation, both dry and wet helium were used. The wet helium was obtained by bubbling dry helium through water prior to its use. The partial pressure of water vapor at equilibrium with pure water is 0.03 atm at 298 K. However, the actual partial pressure of moisture in the shielding gas due to bubbling was found to be 0.008 atm based on the weight loss of the water from the bubbler. The flow rate of the shielding gas was set to be 200 ft<sup>3</sup>/h (5.66 m<sup>3</sup>/h) for both dry and wet helium.

The weld geometry was determined using optical microscopy and computer-assisted image analysis. Porosity was characterized by radiography utilizing X-ray source, optical microscopy and

SEM. The radiographs of the welded samples were obtained using 30 kV and 2.5 mA with 38 s exposure.

The concentration profiles of magnesium were determined using a Camebax SX50 electron microprobe, operated at 15 kV and with about 12 mA beam current. In order to obtain the spatial varia-

Table 1 — Chemical Composition of Aluminum Alloys 5182 and 5754

Material	Mg	Si	Mn	Zn
5182	4.44	0.20	0.35	0.07
5754	2.82	0.30	0.45	0.02

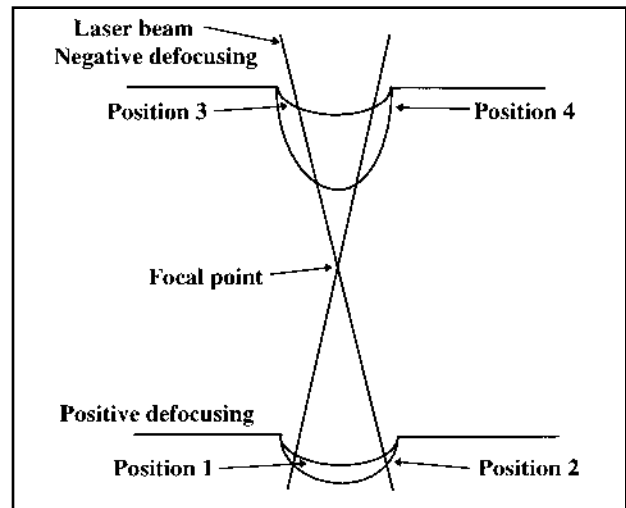


Fig. 4 — Schematic diagram showing interaction of the laser beam with the liquid surface at positive and negative defocusing positions. At positive defocusing, the beam power density decreases with the deepening of the cavity, restricting the growth of the cavity. At negative defocusing, the beam power density increases with the deepening of the cavity, resulting in a deeper keyhole.

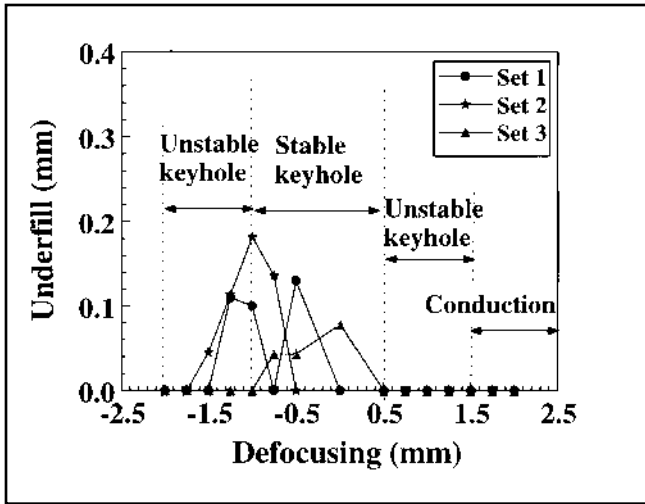


Fig. 5 — Underfill at the root of the weld pool of Alloy 5182 for several defocus values. Nominal power 3 kW, welding speed 250 in./min (105.8 mm/s) and shielding gas flow rate 200 ft<sup>3</sup>/h (5.66 m<sup>3</sup>/h) of helium.

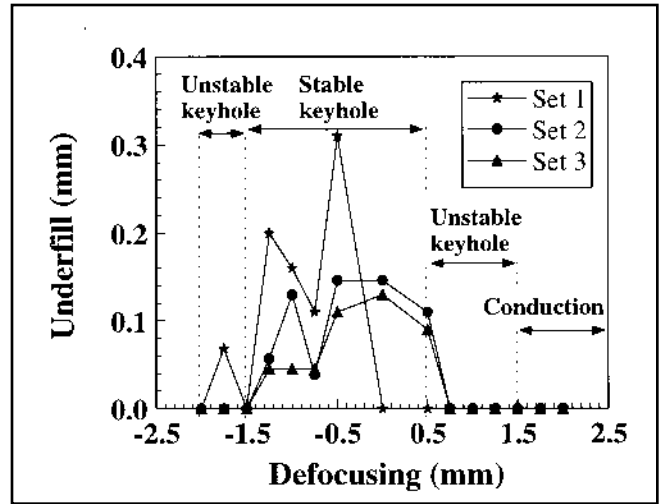


Fig. 6 — Underfill at the root of the weld pool of Alloy 5754 for several defocus values. Nominal power 3 kW, welding speed 150 in./min (63.5 mm/s) and shielding gas flow rate 200 ft<sup>3</sup>/h (5.66 m<sup>3</sup>/h) of helium.

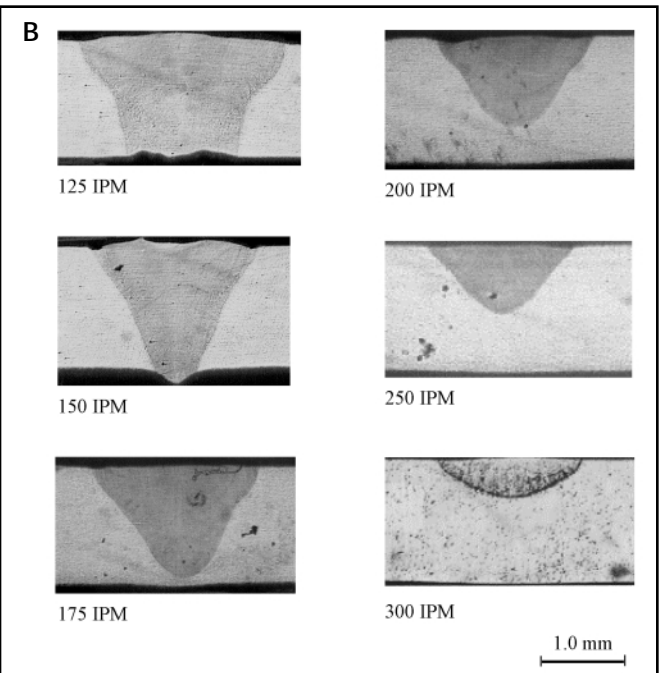
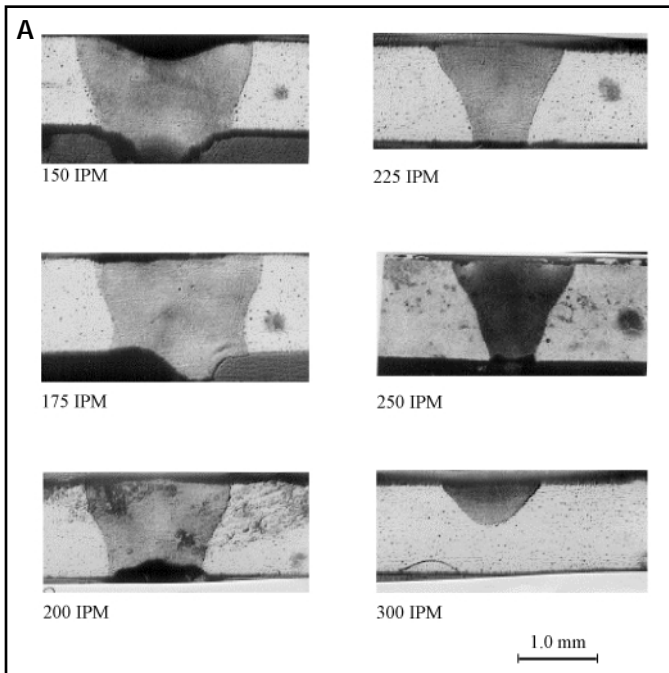


Fig. 7 — A — Cross sections of Alloy 5182 welds obtained with a focused beam for various welding speeds. Nominal power 3 kW and shielding gas flow rate 200 ft<sup>3</sup>/h (5.66 m<sup>3</sup>/h) of helium; B — cross sections of Alloy 5754 welds obtained with a focused beam for various welding speeds. Nominal power 3 kW and shielding gas flow rate 200 ft<sup>3</sup>/h (5.66 m<sup>3</sup>/h) of helium.

tion of concentration in the bulk weld metal and eliminate the effect of interdendritic segregation, the signal for each data point was averaged from a 45 x 55 μm area. The overall change in magnesium concentration owing to welding was calculated from the average composition of the fusion zone.

## Results and Discussion

### Weld Pool Geometry and Underfill

The fusion zone cross sections produced by laser welding of Alloys 5182

and 5754 at different defocusing are shown in Fig. 2. No crack was observed in the welds under the optical microscope. The depth of penetration as a function of defocusing for the welds is given in Fig. 3. It is observed from Figs. 2 and 3 that when welding was performed using a focused beam, a high depth of penetration, characteristic of the keyhole mode of welding, was obtained. On the other hand, when highly defocused beams were used, the depth of penetration was low and the weld pool shapes were characteristic of the conduction mode of welding. When the power den-

sity was near the threshold for keyhole formation, the mode of welding was not reproducible and pool shapes characteristic of either the keyhole or the conduction mode were observed in various cross sections of the same welded sample. In this range, the keyhole was believed to be unstable due to the occurrences of small disturbances within the system, which led to collapse of the keyhole. For example, this behavior was observed for Alloy 5182 when the extent of defocusing was in the range of -1.0 to -2.0 mm and +0.5 to +1.5 mm, as shown in Fig. 3. This figure also shows similar behavior

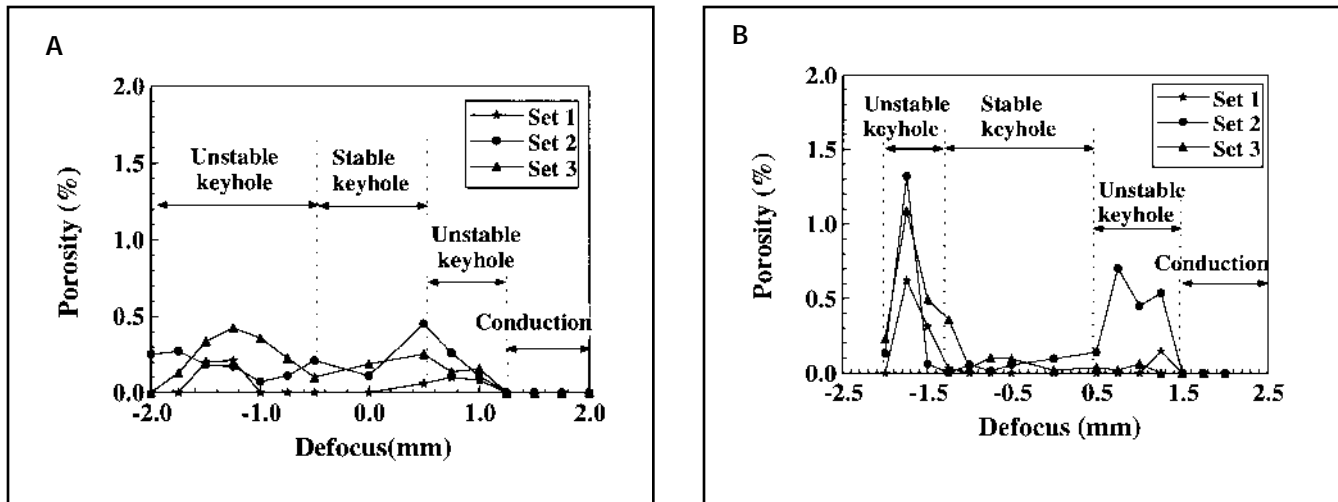


Fig. 8 — Porosity produced at several defocus values. A — 5182; B — 5754. Nominal power 3 kW, welding speeds 250 in./min (105.8 mm/s) and 150 in./min (63.5 mm/s) for Alloys 5182 and 5754, respectively, and shielding gas flow rate 200 ft<sup>3</sup>/h (5.66 m<sup>3</sup>/h) of helium.

for the welding of Alloy 5754 in the range of -1.5 to -2.0 mm and +0.5 to +1.5 mm defocusing. The corresponding estimated laser power densities on the specimen surface were  $8.4 \times 10^5$ ,  $6.7 \times 10^5$ ,  $5.0 \times 10^5$  and  $3.7 \times 10^5$  W/cm<sup>2</sup> for  $\pm 0.5$ ,  $\pm 1.0$ ,  $\pm 1.5$  and  $\pm 2.0$  mm defocusing, respectively.

Figures 2 and 3 show the weld pool size at negative defocusing is larger than that for the same extent of positive defocusing. Arata and coworkers (Ref. 38) also observed larger pool size at negative defocusing. The pool size difference can be explained by considering the interaction of the beam with the liquid weld pool surface (Ref. 38). Near the threshold power density for keyhole formation, the liquid surface is depressed by the recoil force of evaporation, and a shallow depression is produced. As shown in Fig. 4, for positive defocusing, the beam is divergent and the depression moves the liquid surface away from the focal point. As a result, the power density decreases as the liquid surface moves from position 1 to position 2, as shown in this figure. Since the beam power density is near the threshold value, it would decrease below that value if the cavity were to grow any further. Thus, positive defocusing restricts the cavity from further growth. In contrast, at negative defocusing, the beam is convergent and the depression of the liquid surface exposes the bottom surface to a higher power density. Exposure of the liquid surface to progressively higher power density allows the cavity to grow deeper (from position 3 to position 4 in Fig. 4). Thus, once a shallow keyhole is produced at negative defocusing, it has a tendency to grow into a deep keyhole and consequently produce a large weld pool.

The extent of defocusing had pronounced influence on underfill forma-

tion, which was measured by the maximum linear depth of depression at the root of the weld. The influence of defocusing on underfill formation was measured from the cross sections of the welds conducted at several defocus values for three sets of experiments, and the results are presented in Figs. 5 and 6 for Alloys 5182 and 5754, respectively. The underfill was observed in the range from -2.0 mm to +0.5 mm of defocusing in Alloy 5182 and in the range from -1.5 mm to +0.5 mm of defocusing in Alloy 5754. Because of the complexity of the physical phenomena involved, a quantitative understanding of the evolution of the underfill at the bottom of the weld pool does not exist at the present time. In welds with underfill, spattered metal particles were collected in the back-plate groove below the weld region. This behavior indicates that the underfill was caused by expulsion of the molten metal. When the vapor pressure in the keyhole increases above a certain level, it may open a conduit at the bottom of the weld and the flow of gas can carry some liquid metal. As the laser beam moves forward, underfill may form if the molten metal can not refill all the depressions at the bottom of the weld.

The control of the laser power density by changing the extent of laser beam defocusing did not result in welds completely free of underfill. However, sharp or deep notches, which are harmful to the mechanical properties of the weld, were not observed in the cross section of the welds as a result of underfill.

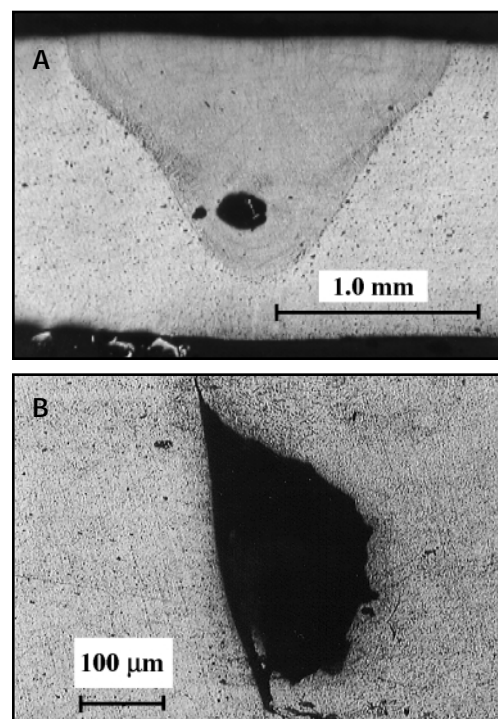


Fig. 9 — Cross sections of the welds of Alloy 5754 showing characteristic macroporosity produced by the instability of the keyhole. A — Spherical porosity; B — irregular-shaped porosity. Nominal power 3 kW, welding speed 150 in./min (63.5 mm/s) and shielding gas flow rate 200 in./min (5.66 m<sup>3</sup>/h) of helium.

Figure 7 depicts the fusion zone cross sections at different welding speeds. It is observed that the keyhole mode of welding with complete penetration was achieved at welding speeds up to 150 in./min (63.5 mm/s) for Alloy 5754 and up to 250 in./min (105.8 mm/s) for Alloy 5182. At higher speeds, nonuniform penetration was observed, and the keyhole

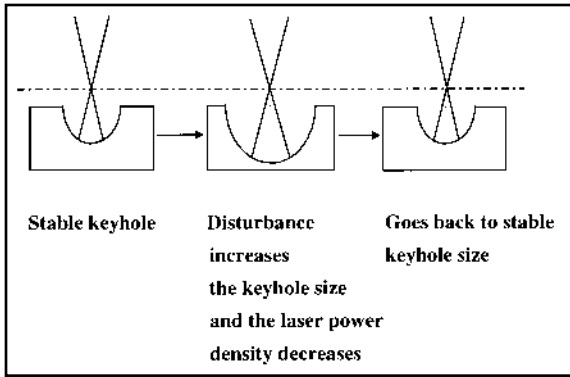


Fig. 10 — Self-stabilizing effect of positively defocused laser beam. The graph shows if the keyhole expands due to disturbance in the system, the laser power density decreases due to the increased beam-keyhole interaction area at the bottom of the keyhole. As a result, the keyhole returns back to its stable size. Similarly, if the keyhole shrinks due to disturbance, the laser power density increases. This increase opposes shrinking of the keyhole.

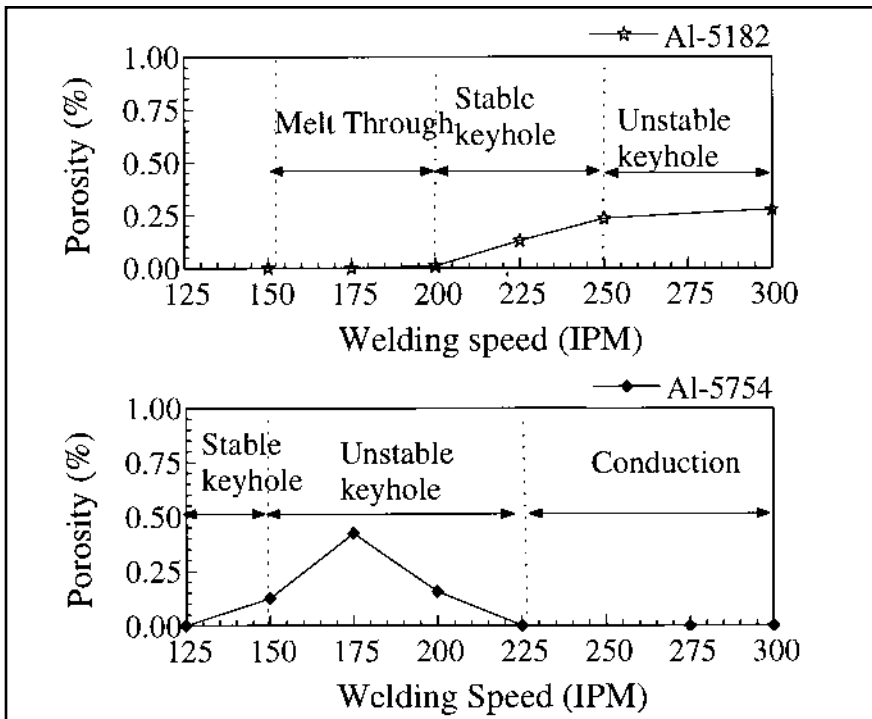


Fig. 11 — Influence of welding speed on pore formation during laser welding of aluminum Alloys 5182 and 5754 using a focused beam. Nominal power 3 kW and shielding gas flow rate 200 ft<sup>3</sup>/h (5.66 m<sup>3</sup>/h) of helium.

was unstable. Melt through was observed at welding speeds of less than 200 in./min (84.7 mm/s) for Alloy 5182 due to excessive heat input.

#### Porosity

Two types of porosity are common in the welding of aluminum alloys. Pores with diameters larger than 0.2 mm, which can be observed by radiography, are called macropores. On the other

hand, pores with diameters of several micrometers, which can only be observed by optical microscopy or SEM, are called micropores. Therefore, both radiography and microscopy were used to characterize porosity in the welds.

#### Macroporosity

It was found that the macropores, which are readily detected by radiography, were the main form of porosity in both alloys. Figure 8 shows the amount of macroporosity in the welds. Three sets of experiments are presented for

gen rejection because, as will be discussed below, the high cooling rate during the laser welding would not allow growth of hydrogen-induced pores to reach this size. Therefore, these pores are considered to be entrapped gas bubbles, which were formed due to the unstable collapse of the keyhole. The main constituent of the pores is believed to be the shielding gas. The spherical pore in Fig. 9A was formed as the liquid metal surrounding it solidified uniformly. The irregular-shaped pore in Fig. 9B was formed as the trapped gas bubble was pushed against the solid-liquid interface by the flow of liquid metal.

Kim, *et al.* (Ref. 39), found more porosity to be formed at negative defocusing than at positive defocusing in laser spot welded 6061 aluminum alloy plates. The fusion zone cross sections shown in Fig. 2 indicate for positive defocusing there is a gradual transition from conduction mode to keyhole mode. Here, the weld penetration increases gradually with a change in defocusing. For negative defocusing, the instability of the keyhole is more pronounced in the transition region.

The difference in the keyhole behavior between positive and negative defocusing in the two transition regions can be explained by considering the stability of the keyhole. The keyhole is inherently more stable at positive defocusing, as shown in Fig. 10. In this arrangement, the beam-material interaction area increases as the depth of the keyhole increases. If a disturbance causes the keyhole to expand, the beam-material interaction area also expands, and the resulting lower power density tends to shrink the keyhole. Similarly, any disturbance that tends to shrink the keyhole causes exposure of the keyhole to a higher power density, which, again, opposes the shrinking of the keyhole. Therefore, a positively defocused laser beam tends to oppose any changes from the stable keyhole size. This explains the smooth transition from conduction mode to keyhole mode for a positively defocused laser beam. On the other hand, since the transition from keyhole to conduction mode occurs in the range of -1.5 to -2.0 mm, the focal point is below the bottom of the plate. In this configuration, the keyhole is inherently unstable because the power density increases all the way from the top to the bottom. Therefore, when a disturbance increases the depth of the keyhole, the material is exposed to a even higher power density that, in turn, further increases the keyhole depth. Thus, the observed variation in the weld metal geometry is consistent with instability of the keyhole during the transition from con-

both the alloys. The data indicate that porosity is minimum when welding is conducted in either keyhole or conduction mode. In contrast, high porosity in the weld metal is observed in the transition region where the keyhole is not stable. Therefore, the formation of macroporosity seems to be linked to the instability of the keyhole. Figure 9 shows two types of macropores in the welds. These pores did not form due to hydro-

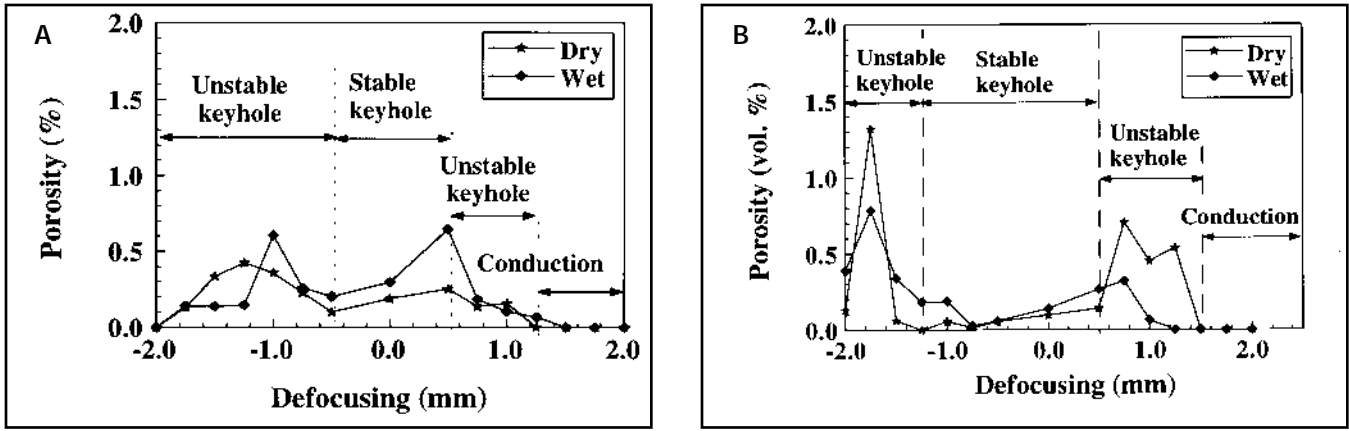


Fig. 12 — Porosity produced at several defocus values with dry and wet helium as the shielding gas. A — Alloy 5182; B— Alloy 5754 . Nominal power 3 kW, welding speeds 250 in./min (105.8 mm/s) and 150 in./min (63.5 mm/s) for Alloys 5182 and 5754, respectively, and shielding gas flow rate 200 ft<sup>3</sup>/h (5.66 m<sup>3</sup>/h) of helium.

duction mode to keyhole mode when the focal point of the beam is below the bottom of the plate.

Figure 11 shows the influence of the welding speed on the extent of porosity. At a given defocusing, as the welding speed is increased, the mode of welding changes from keyhole to conduction regime. During this transition, the keyhole is unstable. It is observed that the highest level of porosity is obtained in regions where an unstable keyhole is formed, whereas porosity is minimized when the welding is conducted in either the stable keyhole or conduction mode. For example, porosity in Alloy 5754 welds was most pronounced between 150 and 200 in./min (63.5 to 84.7 mm/s). At a welding speed of 300 in./min (127 mm/s), the welding takes place in conduction mode and porosity-free welds were obtained. These results, again, indicate that macroporosity is formed due to instability of the keyhole.

Since hydrogen is generally considered to be the main cause of porosity in the welding and casting of aluminum alloys, the role of hydrogen on porosity was examined by using both dry and wet helium as the shielding gas. The volume percent macroporosity in the welds using dry and wet helium as the shielding gas is given in Fig. 12. Comparing the curves for dry and bubbled helium, it is observed that the volume of macroporosity does not significantly change beyond the experimental uncertainty with the addition of moisture to the helium shielding gas. In both cases, the volume percent of macroporosity was the highest when the welding mode was unstable and alternated between keyhole and conduction modes. These experiments provide further evidence that the instability of the keyhole is the main cause of macro-porosity in the welding of Alloys

5182 and 5754. Segregation of hydrogen did not play any significant role in the formation of macroporosity in these welds.

Microporosity

In this investigation, very few micropores were observed in the welds. Figure 13 shows three types of micropores in the welds. Types A and B have a size range between 10 and 30 μm. However, Type A is irregular in shape and Type B is spherical in shape. These two types of porosity are most likely caused by shrinkage or unstable keyhole collapse. Type C is a cluster of randomly distributed small micropores with less than 1 μm size. Among the micropores, Types A and B were more frequently observed than Type C. Type C was observed only in a few samples that were welded using wet helium shielding gas. These pores, with sizes less than 1 μm, are most probably caused by hydrogen rejection from the solid metal.

Hydrogen porosity can be formed by the rejection of hydrogen from the solid due to significant hydrogen solubility difference in the liquid and solid alloy (Ref. 40). Two types of hydrogen porosity are possible in aluminum alloys (Ref. 41). When the hydrogen content in the metal is so high that rejection of the gas from the growing solid raises the equilibrium gas pressure in the liquid to greater than 1 atm (Refs. 42, 43), interdendritic porosity with irregular shape and large size, usually visible to the unaided eye, may form. These features show surface tension forces do not restrain its development. On the

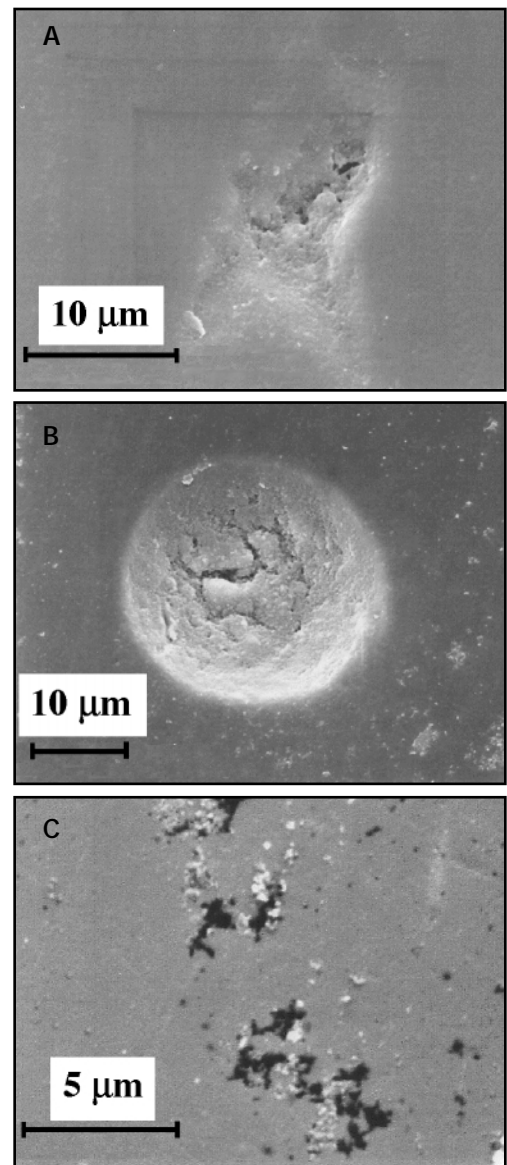


Fig. 13 — Three types of microporosity in Alloy 5754 weld. A — Irregular-shaped porosity; B spherical porosity; C — randomly distributed porosity having spherical or interdendritic shape.





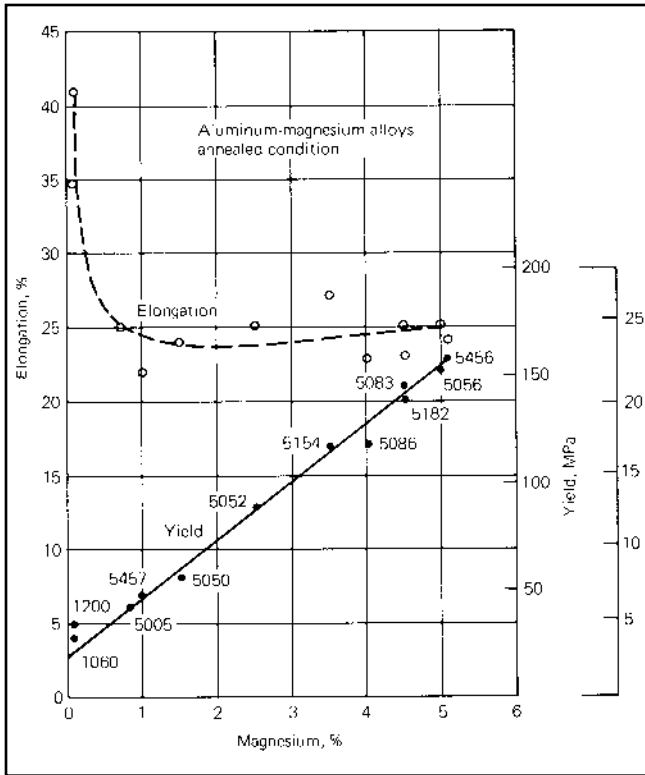


Fig. 16 — Correlation between yield strength, elongation and magnesium concentration for aluminum-magnesium alloys (Ref. 49).

Table 2 — Reduction in Magnesium Concentration in 5182 Aluminum Alloy Welds

Nominal laser power (kW)	3.0				
Welding speed (mm/s)	105.8				
Mode of welding	Conduction				
Defocusing (mm)	+2.0	-2.0	+1.75	-1.75	Keyhole
Reduction in magnesium concentration ( $\Delta\%$ Mg)	1.30	1.20	1.21	1.11	0.74
Changes in magnesium concentration relative to original composition (%)	29.3	27.0	27.3	25.0	16.7

Table 3 — Reduction in Magnesium Concentration in 5754 Aluminum Alloy Welds

Nominal laser power (kW)	3.0				
Welding speed (mm/s)	63.5				
Mode of welding	Conduction				
Defocusing (mm)	+2.0	-2.0	+1.75	-1.75	Keyhole
Reduction in magnesium concentration ( $\Delta\%$ Mg)	0.62	0.59	0.51	0.48	0.22
Changes in magnesium concentration relative to original composition (%)	22.0	20.9	18.1	17.0	7.8

mm defocusing resulted in conduction mode welding. The volumes of metal melted per unit time were 90.1 mm<sup>3</sup>/s and 50.2 mm<sup>3</sup>/s for focused and +2.0 mm defocused beam, respectively. The corresponding magnesium vaporization rates, calculated from the composition change data, were 1.8 and 1.7 mg/s, respectively. Thus, the volume of the molten metal was significantly larger for

focused beam than for +2 mm defocused, while the magnesium vaporization rates were similar in two conditions. As a result, the composition change in the weld with focused beam was less than that with +2 mm defocused beam. Therefore, the keyhole mode of welding results in minimizing changes in magnesium concentration during laser welding.

Welding speed may affect mode of

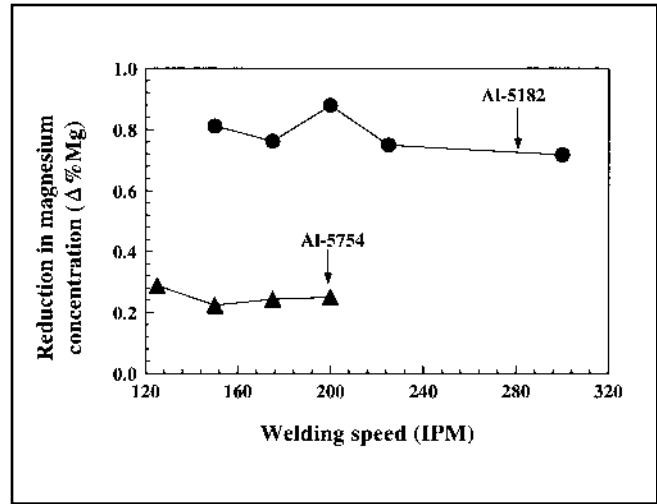


Fig. 17 — Influence of welding speed on the reduction in magnesium concentration during laser welding of aluminum Alloys 5182 and 5754 using a focused beam. Nominal power 3 kW and shielding gas flow rate 200 ft<sup>3</sup>/h (5.66 m<sup>3</sup>/h) of helium.

welding and, consequently, the extent of compositional change in the weld metal. However, when the welding speeds were chosen to maintain the keyhole mode of welding, the compositional change did not vary significantly as shown in Fig. 17. For the welding conditions shown in Fig. 17, the size of the weld pool did not vary significantly to cause major changes in magnesium concentration. At very high welding speeds, the welding mode changes to conduction mode, which leads to more pronounced changes in the magnesium concentration due to much smaller volume of the weld pool. This change occurs, for example, at welding speeds above 275 in./min (116 mm/s) for Alloy 5754. Therefore, a welding speed should be selected to achieve the keyhole mode of welding where possible to minimize the change in magnesium concentration.

### Summary and Conclusions

Porosity and underfill formation and magnesium concentration change during Nd:YAG laser welding of aluminum alloys 5182 and 5754 were studied. The main conclusions are as follows:

- 1) When the welding parameters were close to those for the transition between the keyhole and the conduction modes, pores with diameters larger than 0.20 mm were commonly observed in the weld metal. The macroporosity in the welds resulted from the instability of the keyhole.
- 2) The instability of the keyhole and pore formation can be minimized by controlling the laser beam defocusing and welding speed. The keyhole is more

